



You have downloaded a document from
RE-BUŚ
repository of the University of Silesia in Katowice

Title: Modeling of spatial variations of growth within apical domes by means of the growth tensor. Pt. 1. Growth specified on dome axis

Author: Zygmunt Hejnowicz, Jerzy Nakielski, Krystyna Hejnowicz

Citation style: Hejnowicz Zygmunt, Nakielski Jerzy, Hejnowicz Krystyna. (1984). Modeling of spatial variations of growth within apical domes by means of the growth tensor. Pt. 1. Growth specified on dome axis. "Acta Societatis Botanicorum Poloniae" (Vol. 53, nr 1 (1984) s. 17-28).



Uznanie autorstwa - Licencja ta pozwala na kopiowanie, zmienianie, rozprowadzanie, przedstawianie i wykonywanie utworu jedynie pod warunkiem oznaczenia autorstwa.



UNIwersYTET ŚLĄSKI
W KATOWICACH



Biblioteka
Uniwersytetu Śląskiego



Ministerstwo Nauki
i Szkolnictwa Wyższego

Modeling of spatial variations of growth within apical domes by means of the growth tensor. I. Growth specified on dome axis

ZYGMUNT HEJNOWICZ, JERZY NAKIELSKI, KRYSZYNA HEJNOWICZ

Department of Biophysics and Cell Biology, Silesian University,
Jagiellońska 28, 40-032 Katowice, Poland

(Received: June 6, 1983. Accepted: October 10, 1983)

Abstract

By using the growth tensor and a natural curvilinear coordinate system for description of the distribution of growth in plant organs, three geometric types of shoot apical domes (parabolic, elliptical and hyperbolic) were modeled. It was assumed that apical dome geometry remains unchanged during growth and that the natural coordinate systems are paraboloidal and prolate spheroidal. Two variants of the displacement velocity fields \underline{V} were considered. One variant is specified by a constant relative elemental rate of growth along the axis of the dome. The second is specified by a rate increasing proportionally with distance from the geometric focus of the coordinate systems (and the apical dome). The growth tensor was used to calculate spatial variations of growth rates for each variant of each dome type. There is in both variants a clear tendency toward lower growth rates in the distal region of the dome. A basic condition for the existence of a tunica is met.

Key words: apical dome, growth tensor, growth variations

INTRODUCTION

Symplastic growth is a tensorial attribute of plant organs (Hejnowicz and Romberger 1984, Hejnowicz 1984). The growth tensor is a covariant derivative of the displacement velocity field in the organ. Linear relative elemental rate of growth in a direction s , $REG_{l(s)}$, can be calculated as the double inner product of the growth tensor expressed in physical components and the unit vector pointing in direction s . The relative elemental rate of growth in volume, REG_{vol} , is given by the sum of diagonal components of the growth tensor. Another important property of the growth tensor derives from its eigenvectors. To appreciate this term, observe that when the growth tensor is multiplied by a vector, i.e. the tensor "acts" on a directed linear element in the organ, a new vector appears which in general has a direction and magnitude different from the original one. However, there are

always three orthogonal vectors, called eigenvectors of the tensor, at each position, which maintain their original directions though the magnitude is changed (if the growth is isotropic all vectors maintain their direction). The directions of the eigenvectors are termed the principal directions of growth. If the growth tensor is multiplied by a unit vector of variable direction, the magnitude of the resulting vector attains an extreme value, either maximal or minimal, in the principal directions. These extreme $RERG_i$ values are called principal growth rates. They pertain to the principal directions of growth, which are mutually orthogonal. The principal directions of growth can be associated with each positional point within an organ, and short line segments corresponding to these directions can be joined to form a network of orthogonal trajectories. These trajectories represent a natural coordinate system most favourable for dynamic description of a growing organ (Hejnowicz 1984). The ratio of a pair of principal growth rates quantitatively specifies the directionality of growth in the corresponding plane. The more this ratio deviates from 1 the more pronounced is the anisotropy of growth. We refer to this ratio as to anisotropy ratio (Erickson 1976).

Our aim is to illustrate use of the growth tensor and the natural coordinate system, as indicated by the title of this paper, in relatively simple cases of growing organs, namely in apical domes of different chape but growing in such a way that the shape is steady. We will consider three types of apical dome: (A) parabolic, (B) elliptic, and (C) hyperbolic (Fig. 1) assuming that the natural coordinate systems for these domes are paraboloidal (u, v, φ) for A, and are two variants of prolate spheroidal (ξ, η, φ) for B and C.

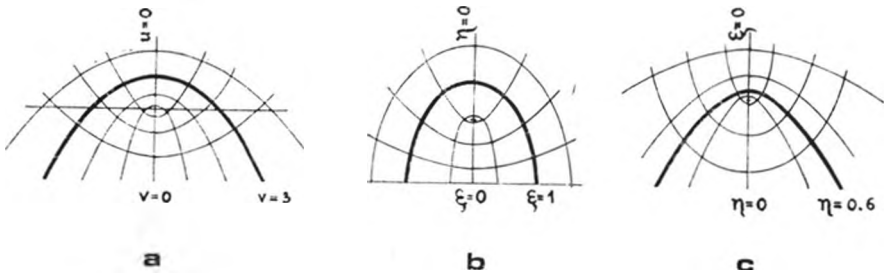


Fig. 1. Schemes of the natural coordinate systems for apical domes considered in this paper. It is assumed that the thicker periclinal coordinate curve represents the surface of the dome. a — paraboloidal coordinate system, b and c — two variants of prolate spheroidal coordinate system: b for elliptic dome, c for hyperbolic dome

THE GROWTH TENSOR IN PHYSICAL COMPONENTS, GENERAL FORM

The growth tensor in physical components can be obtained either by converting into physical components the covariant derivative of the displacement velocity field, V , or directly from the dyadic ∇V (Hejnowicz and Romberger 1984). We omit the procedure of deriving the tensor, and write the final form of the tensor taking into account the simplification resulting from the assumption that we are

considering apical domes that grow with steady geometry. This simplification requires that there be only one non-zero component in the vector \underline{V} , namely that corresponding to the periclinal coordinate lines (which are meridional on the surface) (Hejnowicz 1984). Thus, there is only V_u in the parabolic dome ($V_v = V_w = 0$), only V_n in the elliptic dome, and only V_ξ in the hyperbolic dome. The growth tensor in the general form, i.e. without specification of the field $V_{periclinal}$ is:

(A) Parabolic dome:*

$$\frac{1}{\sqrt{u^2 + v^2}} \begin{vmatrix} \frac{\delta V_u}{\delta u} & -\frac{vV_u}{u^2 + v^2} & 0 \\ \frac{\delta V_u}{\delta v} & \frac{uV_u}{u^2 + v^2} & 0 \\ 0 & 0 & \frac{V_u}{u} \end{vmatrix}$$

(B) Elliptic dome:

$$\frac{1}{\sqrt{\sin^2 h^2 \xi + \sin^2 \eta}} \begin{vmatrix} \frac{V_n \sin \eta \cos \eta}{\sin^2 h^2 \xi + \sin^2 \eta} & \frac{\delta V_n}{\delta \xi} & 0 \\ \frac{V_n \sin h\xi \cos h\xi}{\sin^2 h^2 \xi + \sin^2 \eta} & \frac{\delta V_n}{\delta \eta} & 0 \\ 0 & 0 & \frac{V_n \cos \eta}{\sin \eta} \end{vmatrix}$$

(C) Hyperbolic dome:

$$\frac{1}{\sqrt{\sin^2 h^2 \xi + \sin^2 \eta}} \begin{vmatrix} \frac{\delta V_\xi}{\delta \xi} & -\frac{V_\xi \sin \eta \cos \eta}{\sin^2 h^2 \xi + \sin^2 \eta} & 0 \\ \frac{\delta V_\xi}{\delta \eta} & \frac{V_\xi \sin h\xi \cos h\xi}{\sin^2 h^2 \xi + \sin^2 \eta} & 0 \\ 0 & 0 & \frac{V_\xi \cos h\xi}{\sin h\xi} \end{vmatrix}$$

Each form of the growth tensor given above is in a natural coordinate system, thus the diagonal components represent the principal growth rates. A nondiagonal component T_{pq} , $p \neq q$, represents the angular velocity of the rotation around an axis normal to the plane pq . It is not directly evident from the general form of the growth tensor that the nondiagonal components are skew-symmetric (which is the condition for their representing rotation velocities), however, this field \underline{V} must be such as to guarantee this property.

* the symbol $\frac{\delta}{\delta}$ denotes partial derivative

METHODS OF CALCULATIONS

One should observe that the field V cannot be defined without restriction because the growth must be compatible, i.e. the various organ parts must remain joined together during growth. The principles of V field specification are given in a previous paper (Hejnowicz 1984). If $V_{\text{periclinal}}$, termed V_1 , is specified along one coordinate line u_1 , i.e. $u_2=a$, and $V_1=V_1(u_1, u_2=a)^*$, the general equation for V_1 is $V_1 = \frac{h_1}{\tilde{h}_1} \tilde{V}_1$ where h_1 is the scale factor in the direction tangent to the u_1 curve and is given in its general form, i.e. $h_1=h_1(u_1, u_2)$, while \tilde{h}_1 and \tilde{V}_1 are the scale factor and displacement velocity along the coordinate line defined by $u_2=a$.

The scale factors for different natural coordinate systems are given in a previous paper (Hejnowicz 1984), for instance, for the parabolic dome $h_1=\sqrt{u^2+v^2}$, and \tilde{h}_1 on the dome axis ($v=0$, there) is $\tilde{h}_1=\sqrt{u^2}=u$.

The growth tensor was utilised to calculate the variation of REG_i and REG_{vol} by means of a RIAD 32 computer.

The linear relative elemental rates of growth, REG_i , in different directions differing by 10° one from the other in a chosen plane, were evaluated by the double product of the growth tensor and the unit vector in a particular direction at the considered point.

Values of REG_i in all possible directions from a considered point determine a closed surface such as the "peanut-shaped" representations in Fig. 2. The extremal values lie along the principal directions, which can be denoted as periclinal (P), anticlinal (A), and latitudinal (L). These directions define three orthogonal planes which are shown in the Fig. 2: axial (AP), tangent to anticlinal surface (AL), and tangent to periclinal surface (PL). Values of REG_i are displayed in the form of two-dimensional plots of REG_i around a number of points lying on the axial plane (Figs. 3-5, 7, 8, 10). The plots are in the planes AP and PL . Examples of plots in the plane AL and in the plane transverse to dome axis are in Figs. 3b and 4b. The latter plane is determined by the latitudinal and radial directions and is denoted as the LR plane.

Elongate or bilobate plots indicate anisotropic growth. The long axis of each plot indicates maximal principal growth rate, the short axis (the neck of bilobate plot) indicates the minimal rate (except the map in Fig. 4b which involves only one principal direction).

Plots of REG_i for a given variant are all on the same scale.

The volumetric growth rate, REG_{vol} , was evaluated for points on the axial plane and displayed in the form of regions corresponding to chosen ranges of REG_{vol} . The program SYMAP was used to get map of the regions.

* In case of the apical dome which is a figure of revolution and grows without rotation of the tip, the V -field does not depend upon $u_3=\varphi$. Also the scaling factors do not depend upon φ .

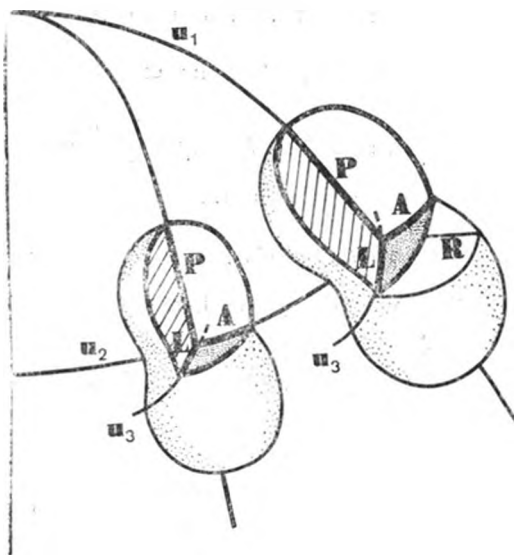


Fig. 2. Imaginary 3-dimensional figures intended to aid visualization of the predicted variation of REG_1 values in all directions from considered points within an apical dome. Each and every point on the surface of one of the "pea-nut-shaped" volumes represents a value of REG_1 in a specific direction from the considered point. Thus only the surface configurations of the "peanut" shapes have significance and points within the volumes have no meaning. Coordinate lines of the "natural" system, u_1 , u_2 , u_3 , which are orthogonal as they pass through the considered point, are indicated. The axis specifying a REG_1 surface in any pair of dimensions are tangent to the corresponding coordinate lines at a considered point, and also specify the principle directions there. The axes determining the REG_1 surface are denoted as P (periclinal), A (anticlinal), and L (latitudinal). R indicates the radial direction with reference to the longitudinal axis of the apex and is not defined in the curvilinear coordinate system. The planes for which REG_1 values are computed and displayed (in the following figures) are PA, PL, AL, and LR

RESULTS

PARABOLIC DOME

Variant A_1 (Fig. 3): $REG_{periclinal}$ is constant on the dome axis

Observe, that the axis consists of two parts, periclinal below the focus and anticlinal above the focus. Our assumption that only $V_{periclinal}$ exists on the axis implies that the REG_1 along the anticlinal part of the axis is zero. This fulfills a necessary condition for existence of a tunica on the apical dome, hence we can consider the anticlinal and periclinal part of the axis as belonging to the tunica and corpus, respectively. The focus represents the vertex of the corpus.

The periclinal part of the axis is defined by $v=0$. From the growth tensor we read that the $REG_{I(v=0)}$ along this part of the axis is $\frac{1}{u} \frac{\delta V_u}{\delta u}$. The condition specifying the variant A_1 is thus: $REG_{I(v=0)} = \frac{1}{u} \frac{\delta V_u}{\delta u} = \text{constant} = k$ (on the axis). From the properties of the natural coordinate system it follows that V_u is a function of u only (Hejnowicz 1984), therefore $\frac{\delta V_u}{\delta u} = \frac{dV_u}{du} = ku$, which by integration leads to the equation for the displacement velocity along the axis: $\vec{V}_u = \frac{1}{2} ku^2$. Thus V_u at different points in the dome is $V_u = \frac{1}{2} ku \sqrt{u^2 + v^2}$. The growth tensor for the variant A_1 thus is:

$$\frac{k}{2} \begin{vmatrix} \frac{2u^2 + v^2}{u^2 + v^2} & -\frac{uv}{u^2 + v^2} & 0 \\ \frac{uv}{u^2 + v^2} & \frac{u^2}{u^2 + v^2} & 0 \\ 0 & 0 & 1 \end{vmatrix}$$

Many of the characteristics of the growing dome can be read from the tensor itself; 1) At the dome vertex the meridional and latitudinal growth rates are equal and amount to $1/2 k$. The ratio of these rates increases from 1 to 2 with increasing distance from the vertex; 2) The ratio of the periclinal to anticlinal growth rates on the axial plane everywhere surpasses 2, thus the directionality of growth in the axial plane is quite pronounced; 3) The latitudinal growth rate is the same everywhere, i.e. each latitudinal linear element increases by k 50% per time unit.

The growth rates in different directions and at different locations for variant A_1 are shown in Figs. 3a-c. It is obvious that the figures produced by REG_I are bilobate everywhere on axial plane (Fig. 3a), however the anisotropy ratio is most pronounced in the distal region close to dome surface. The REG_I figure at a point, on the plane tangent to the anticlinal surface (u constant) at this point, is similar to that on the axial plane in the distal region of the dome (compare Fig. 3b with 3a), however the former tends toward a circle with increasing distance from the tip, while the latter remains bilobate. The REG_I figure at a point, on the plane tangent to periclinal surface (v constant) at this point, is circular in distal region. This means that growth is isotropic in the two dimensions considered there, and tends toward anisotropy (bilobate plots) with increasing distance from the tip (Fig. 3c). The volumetric growth rate (Fig. 3d) varies within a rather narrow range. The lowest rate is in the distal region, the highest in the core of the dome.

Variant A_2 (Fig. 4): $REG_{1\text{periclinal}}$ on the axis increases linearly with physical distance from the focus

The z -component of the physical distance from the focus is: $z = \frac{1}{2} (u^2 - v^2)$ thus, on the axis $z = \frac{1}{2} u^2$ and we can write the condition specifying the variant

A_2 in the form: $\frac{1}{u} \frac{\delta V_u}{\delta u} = kz = k \frac{u^2}{2}$. Upon integrating we obtain $\bar{V}_u = \frac{k}{8} u^4$, and $V_u = \frac{k}{8} u^3 \sqrt{u^2 + v^2}$. The growth tensor for this variant thus is:

$$\frac{k}{8} \begin{vmatrix} \frac{u^2 (4u^2 + 3v^2)}{u^2 + v^2} & -\frac{u^3 v}{\sqrt{u^2 + v^2}} & 0 \\ \frac{u^3 v}{\sqrt{u^2 + v^2}} & \frac{u^4}{u^2 + v^2} & 0 \\ 0 & 0 & u^2 \end{vmatrix}$$

Inspection of this tensor reveals three important facts: (1) At the vertex ($u=0$) linear growth rates vanish in all directions. (2) The ratios of the periclinal to the latitudinal, and of the periclinal to the anticlinal principal growth rates, are everywhere between 3 and 4, and higher than 4, respectively, which indicates appreciable anisotropy of growth. (3) The anticlinal growth rate along the axis is null above the focus, thus this part of the axis belongs to the tunica.

Figures 4a-d consists of maps of growth rate distribution for variant A_2 . The anisotropy of growth on an axial plane and on periclinal surfaces is more pronounced than in variant A_1 . Note that Figs. 3b and 4b represent different planes of REG_{1i} plotting. The REG_{1i} on transverse plane shown in Fig. 4b was calculated according to the formula:

$$REG_{1(trans)} = \frac{v^2}{u^2 + v^2} REG_{1(per)} + \frac{u^2}{u^2 + v^2} REG_{1(ant)} = \frac{1}{8} \frac{u^2}{(u^2 + v^2)^2} (4u^2 v^2 + u^4 + 3v^4).$$

The distal region of low growth rate appears more clearly than in variant A_1 . The borders between regions classified on the basis of volumetric growth rate are oriented anticlinally. The REG_{1i} figures in the very distal region are reduced practically to points and their shapes cannot be discerned. It is easy to show that this figure would be circular at the vertex on the periclinal surface if the variant A_2 were modified so as to have growth rates, in the meridional and latitudinal directions, of certain value greater than 0 at the vertex (in A_2 they equal 0 there). This can be achieved by starting the $REG_{1(u)}$ on the axis not from null as in A_2 , but from a certain positive value, say b . The growth tensor in this subvariant would be:

$$\frac{1}{8} \left| \begin{array}{cc|c} \frac{4ku^4+16bu^2+v^2(3ku^2+8b)}{u^2+v^2} & -\frac{uv(ku^2+8b)}{u^2+v^2} & 0 \\ \frac{uv(ku^2+8b)}{u^2+v^2} & \frac{u^2(ku^2+8b)}{u^2+v^2} & 0 \\ 0 & 0 & ku^2+8b \end{array} \right|$$

It is seen that the meridional and latitudinal principal growth rates at the vertex, $u=0$, $v>0$, are both b , thus their ratio there is 1.

ELLIPTIC DOME

Variant B₁ (Figs. 5 and 6a): $REG_{\text{periclinal}} = REG_1(\eta)$ is constant on the axis

Along the periclinal part of axis $\xi=0$. From the growth tensor in spheroidal coordinates we have on the axis: $REG_1(\eta) = \frac{1}{\sin \eta} \frac{\delta V_\eta}{\delta \eta} = k$ thus $\vec{V} = -k \cos \eta + C$. At the focus $\vec{V}_\eta=0$, $\eta=0$, thus $C=k$. We have thus: $\vec{V}_\eta = k(1 - \cos \eta)$ on the axis, and $V_\eta = \frac{\sqrt{\sin^2 h^2 \xi + \sin^2 \eta}}{\sin \eta} k(1 - \cos \eta)$ in the whole dome. The growth tensor for this variant is thus:

$$k \left| \begin{array}{cc|c} 1 - \frac{\cos \eta \sin h^2 \xi}{(\sin h^2 \xi + \sin^2 \eta)(1 + \cos \eta)} & -\frac{(1 - \cos \eta) \sin h \xi \cos h \xi}{\sin \eta (\sin h^2 \xi + \sin^2 \eta)} & 0 \\ \frac{(1 - \cos \eta) \sin \eta \xi \cos h \xi}{\sin \eta (\sin h^2 \xi + \sin^2 \eta)} & \frac{(1 - \cos \eta) \cos \eta}{\sin h^2 \xi + \sin^2 \eta} & 0 \\ 0 & 0 & \frac{\cos \eta}{1 - \cos \eta} \end{array} \right|$$

Inspection of this growth tensor reveals that both the meridional and the latitudinal principal growth rates attain $\frac{1}{2}$ at the vertex, however, it is difficult to read the ratio of the principal growth rates from the tensor directly. The ratio and variation of growth rates are shown on the maps in Figs. 5a, b and 6a. At the vertex there is isotropy of growth on dome surface, as we would expect. The meridional rate at the vertex is considerable while the anticlinal rate is null, which means that conditions favor development of a tunica. The rate of volumetric growth attains a maximum at the vertex of the corpus (just below the focus). The decrease of REG_{vol} in the basal part of the dome is due to the decrease of REG_1 in anticlinal and latitudinal directions there.

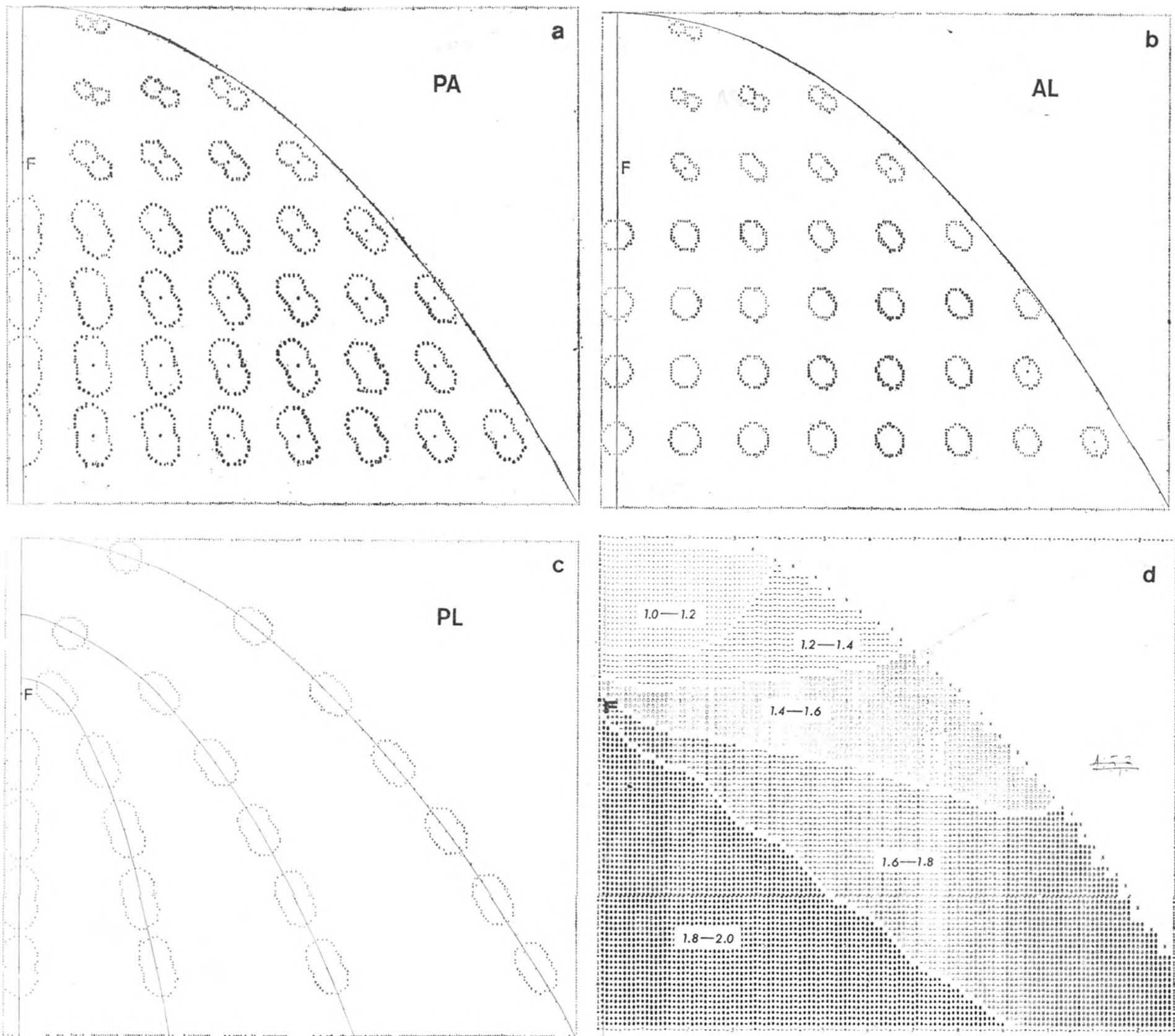


Fig. 3. Spatial and orientational variation of growth rates for variant A_1 . In each figure only half of the axial longisection of the dome is shown, the y -coordinate corresponds to the dome axis. The x -coordinate corresponds to the dome radius. The curvilinear coordinates are not marked, however, the points in Fig. 3c lie along four coordinate lines u ($\nu=0$ i.e. the dome axis, $\nu=1$, $\nu=2$, $\nu=3$). The position of the focus is indicated by the point F. Distances from the vertex and radial distances are plotted in arbitrary units, the same for both coordinates (x and y). a — Plots of REG_1 for plane PA (see Fig. 2); b — Plots of REG_1 for plane AL (the L -direction in the figure is oriented periclinally in result of plot rotation by 90° around A); c — Plots of REG_1 for plane PL (the L -direction in the figure is oriented anticlinally). The units of REG_1 (100% of the growth increment during arbitrary unit time) are the same for all plots. d — Zonation with respect to the REG_{vol} . The numbers indicate the range of values of REG_{vol} in zones shaded with identical symbols. The unit of REG_{vol} is arbitrary, because it represents the increment of volume of a small element at a point during an arbitrary unit time

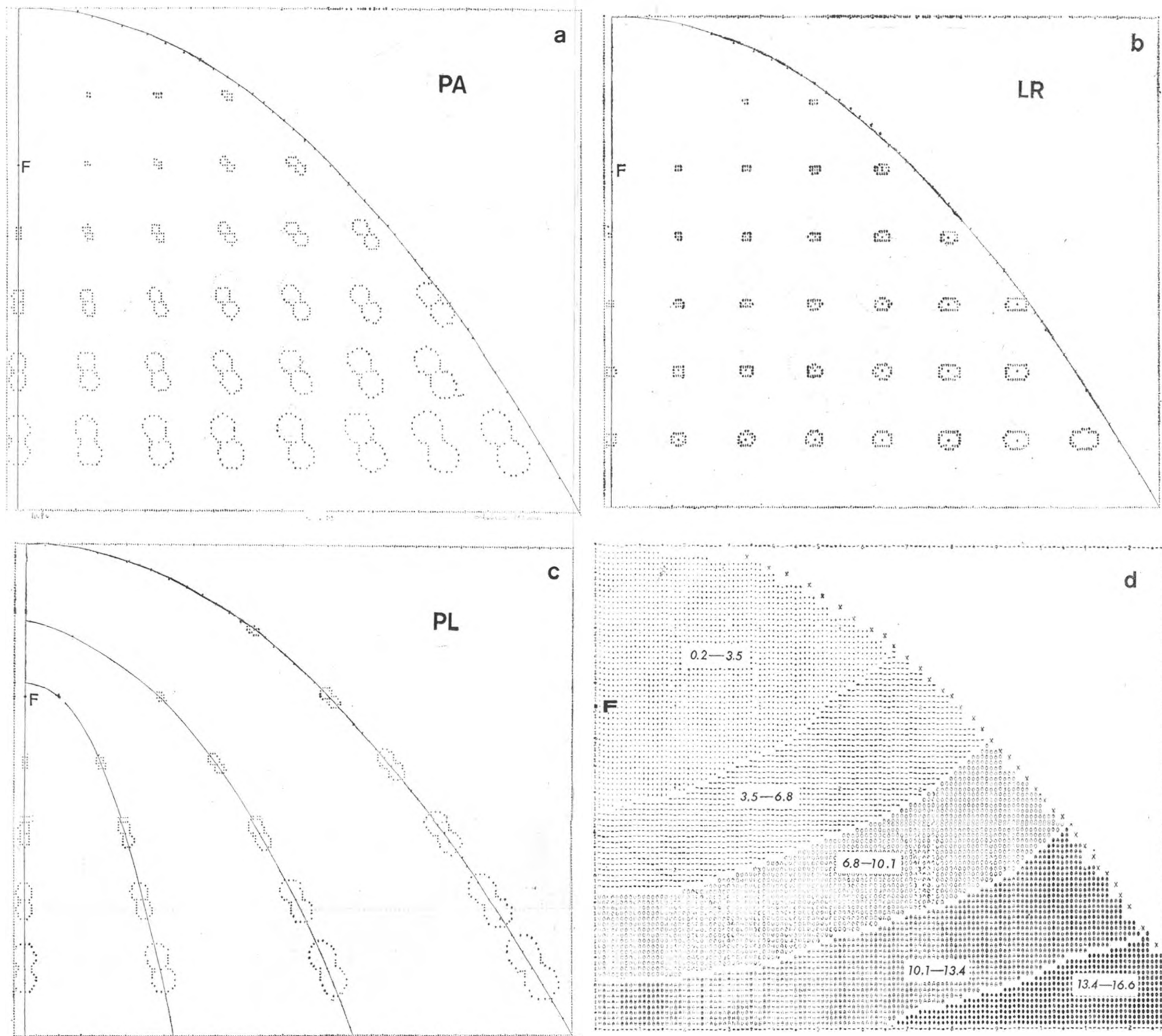


Fig. 4. Spatial and orientational variation of growth rates for the variant A_2 . Explanation as in Figs. 2 and 3, except that the (b) shows $RERG_1$ in the plane LR (transverse to dome axis) instead in the plane AL as in Fig. 3b

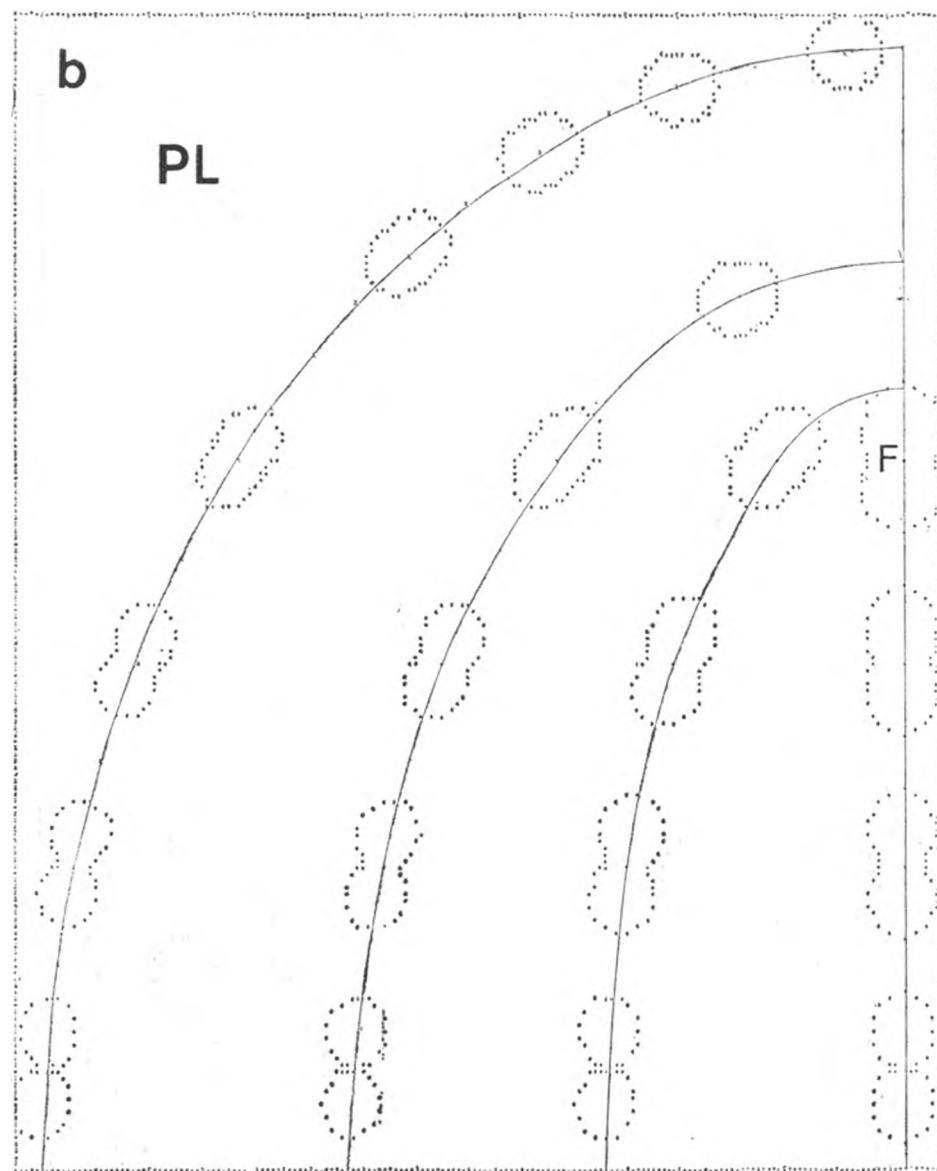
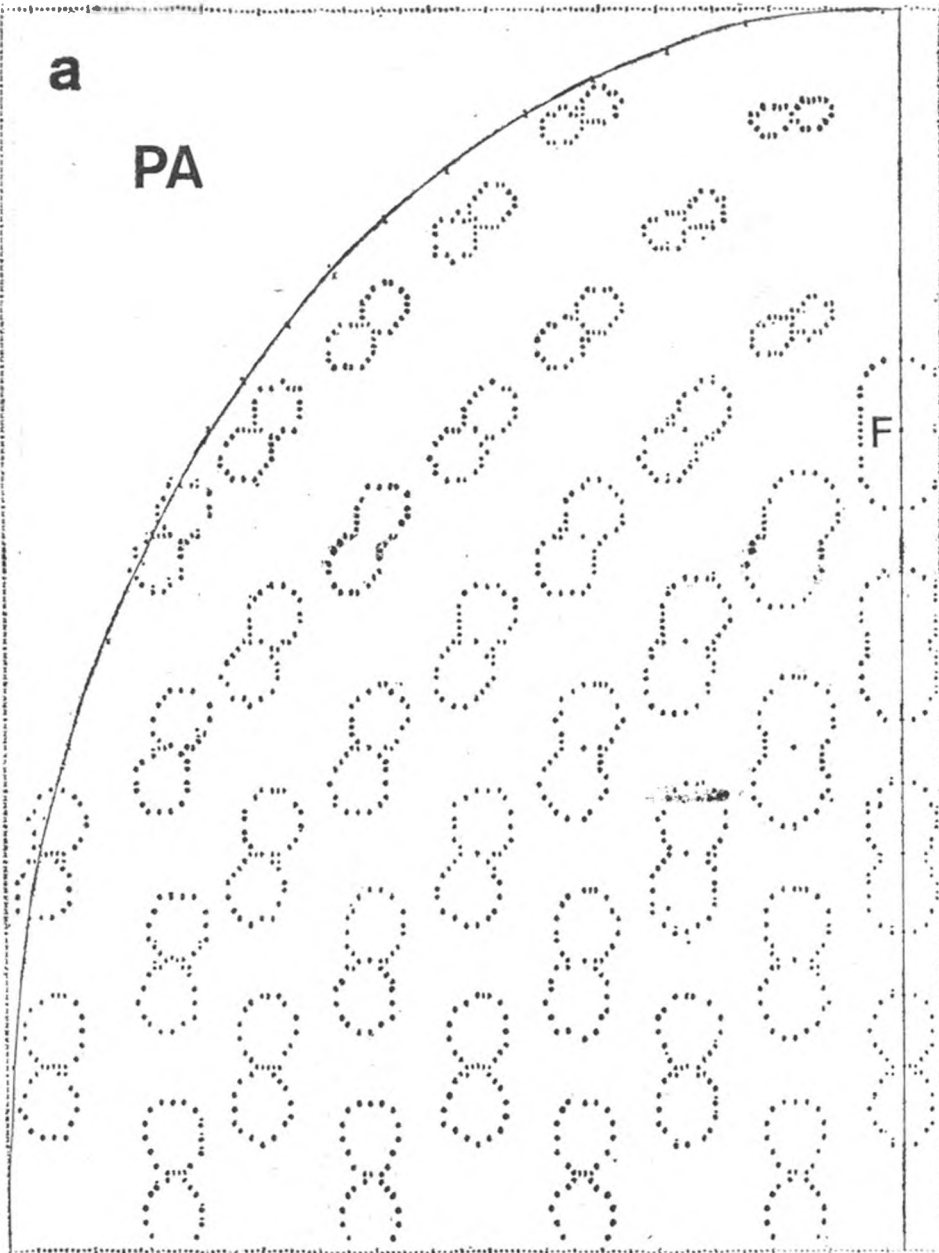


Fig. 5. Spatial and orientational variations of $RERG_1$ for variant B_1 . a — plane PA (axial plane); b — plane tangent to periclinal surface, PL

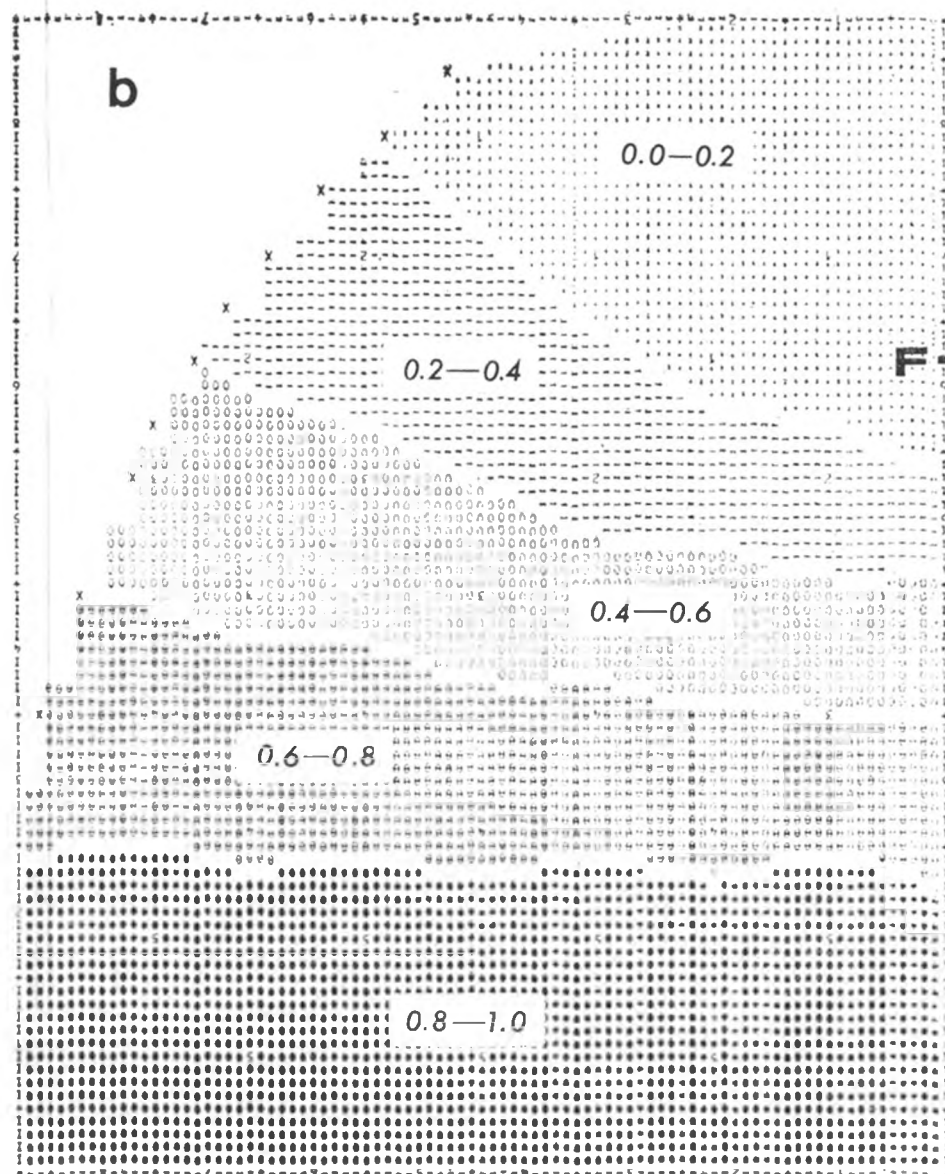
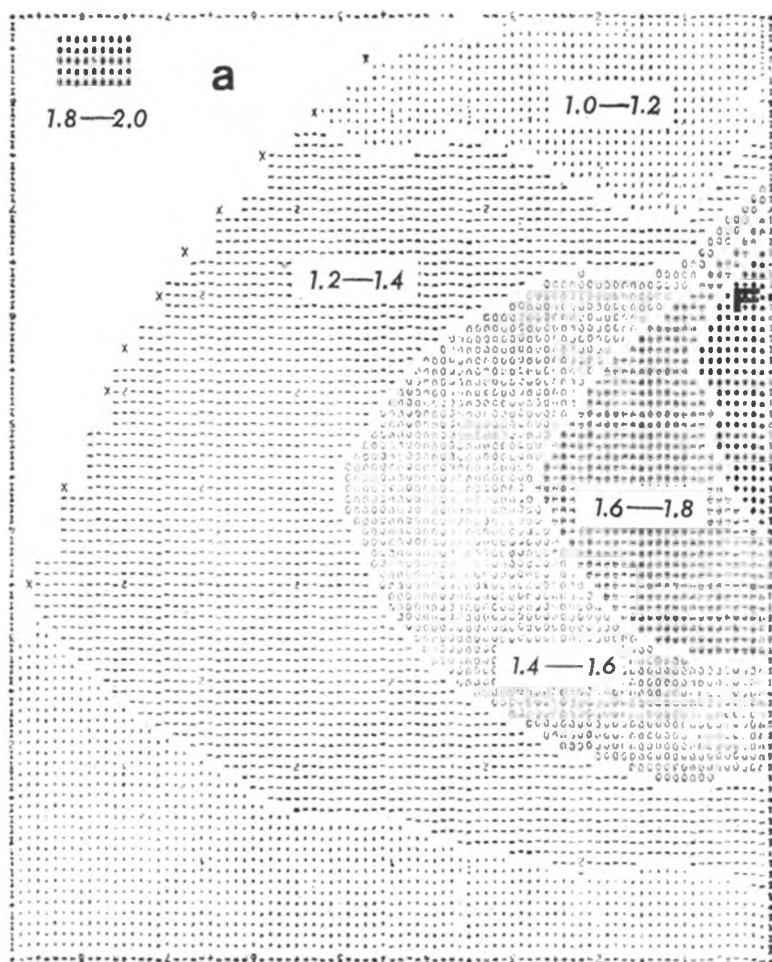


Fig. 6. Regions of $RERG_{vol}$ for variant B_1 (a), and for variant B_2 (b)

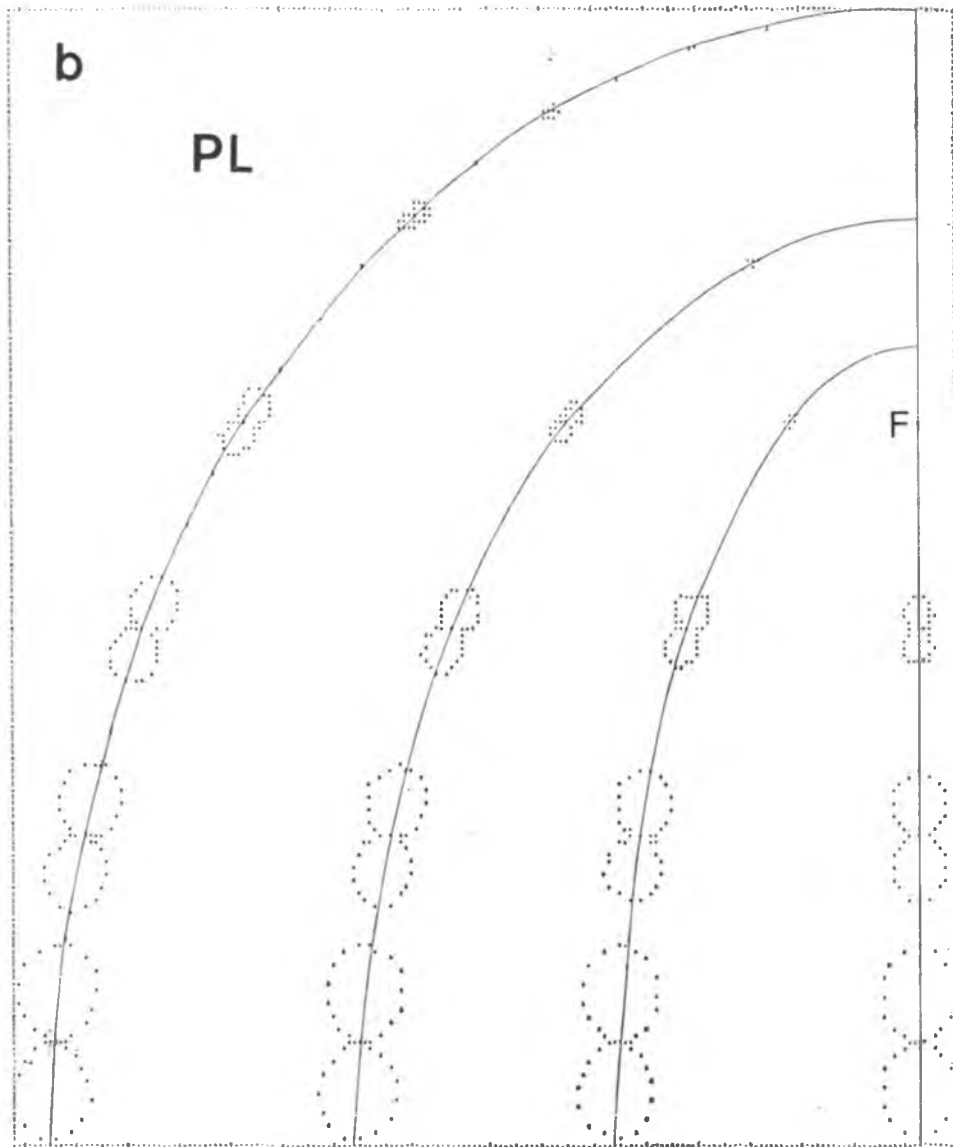
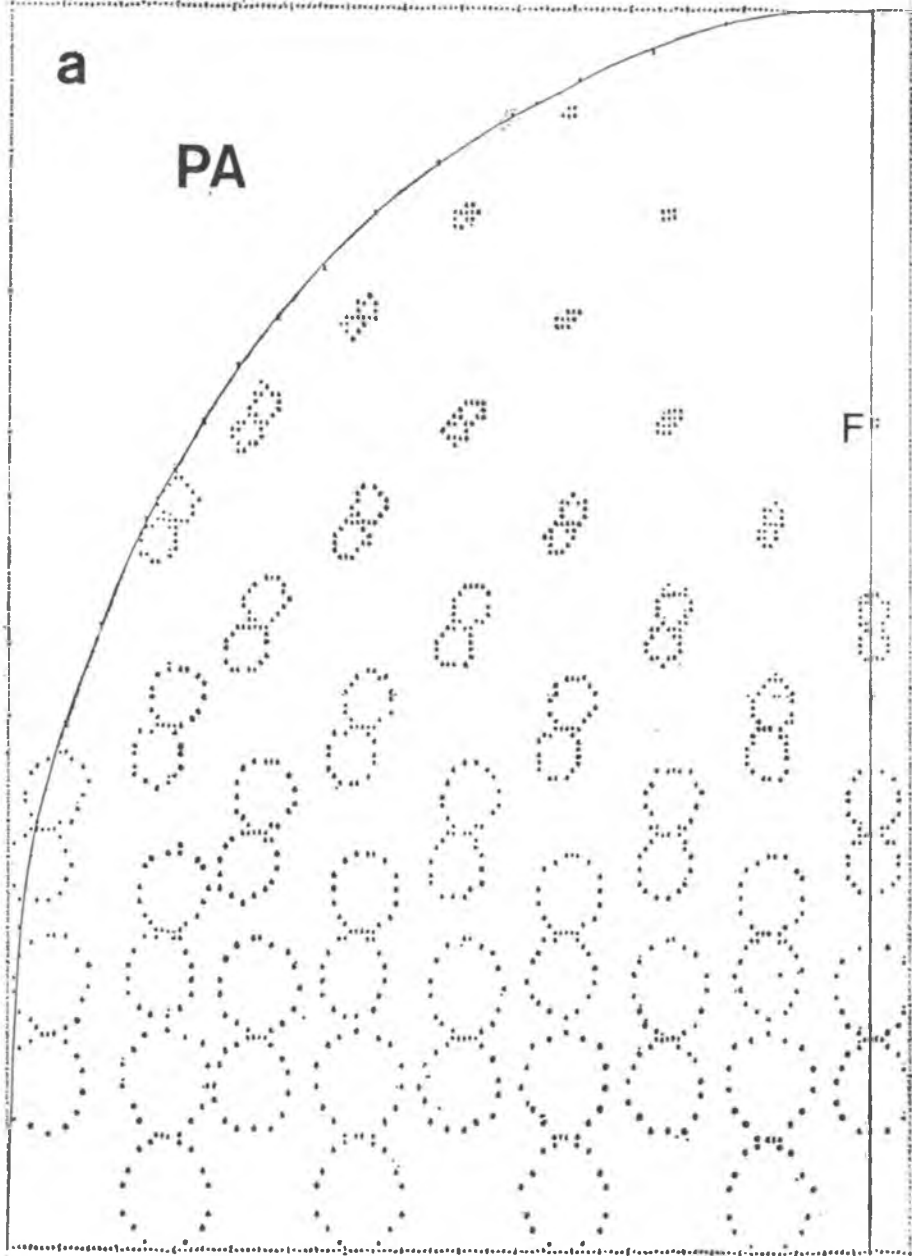


Fig. 7. Spatial and orientational variation of $RERG_1$ for variant B_2 . a — axial plane (PA); b — plane tangent to periclinal surface (PL)

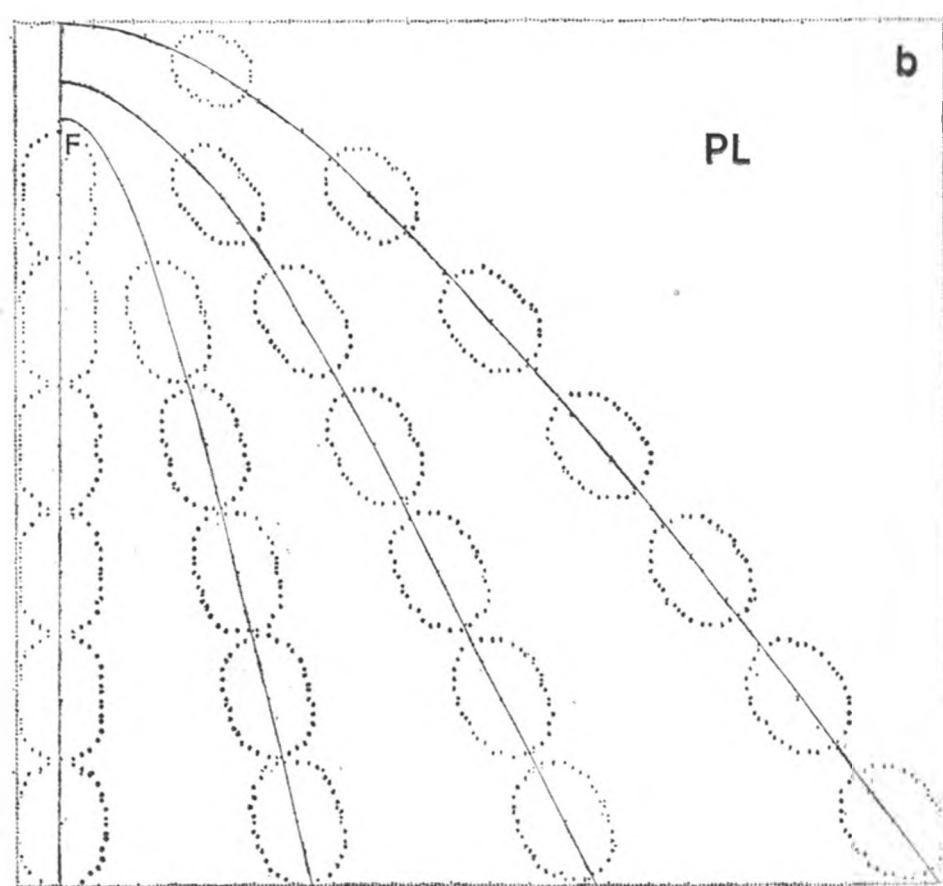
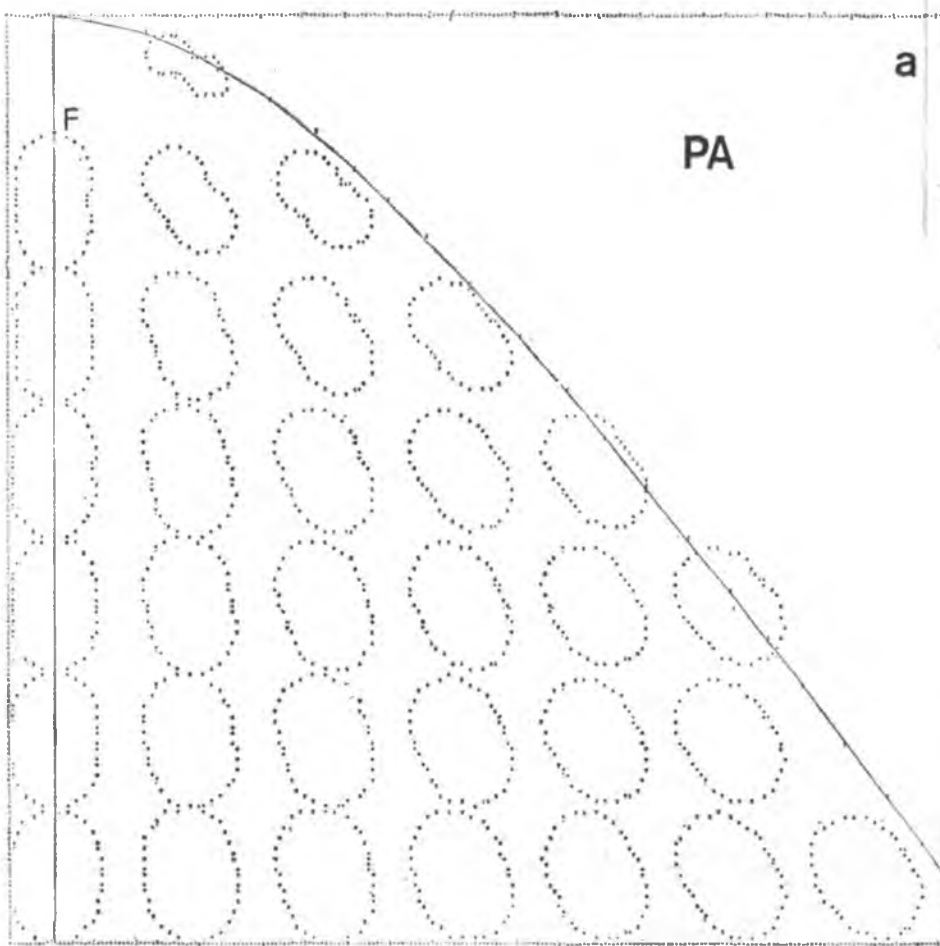


Fig. 8. Spatial and orientational variation of $RERG_1$ for variant C_1

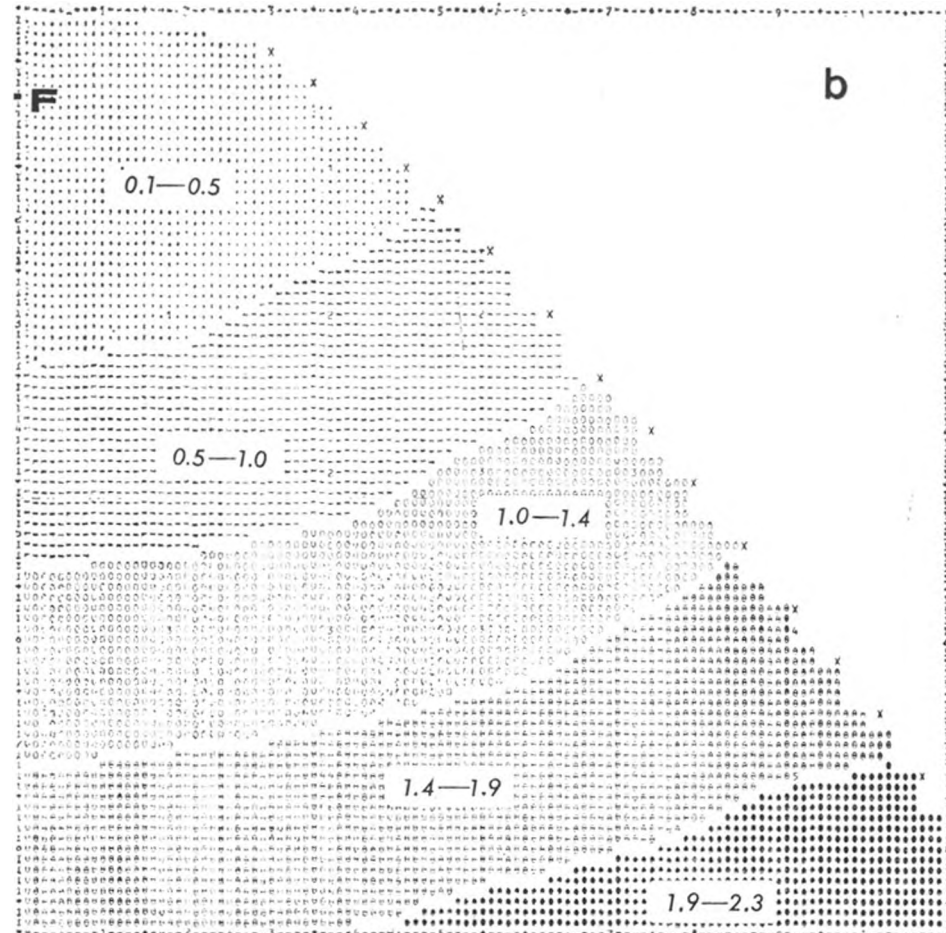
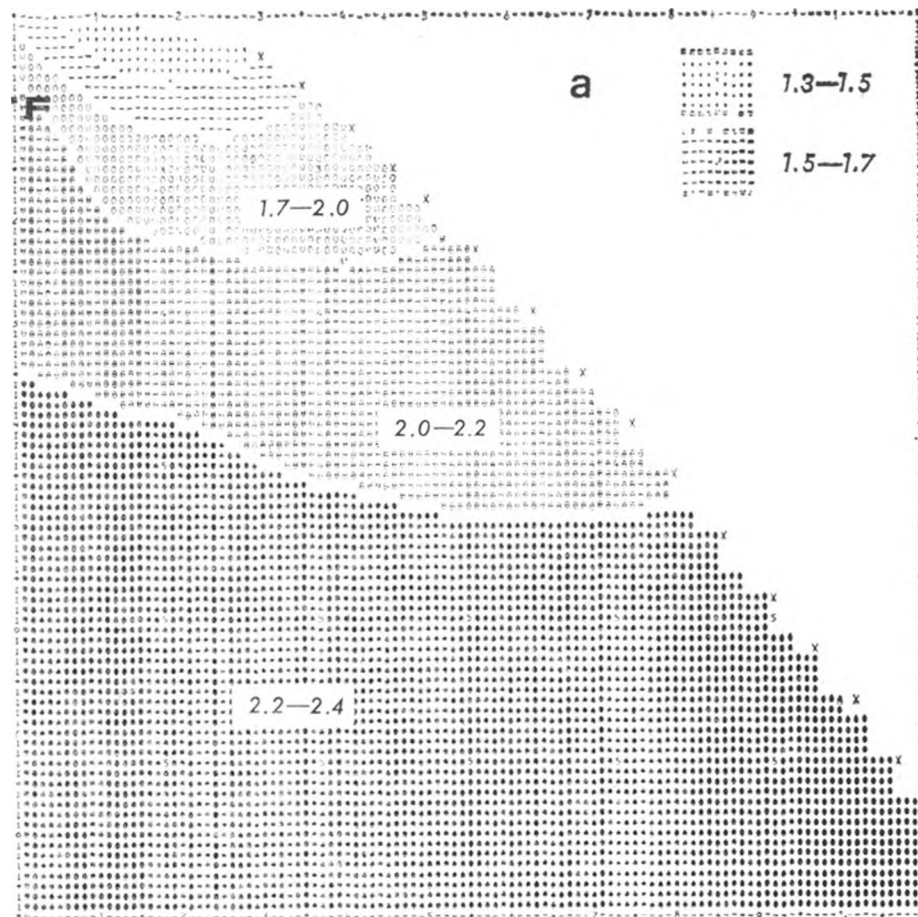


Fig. 9. Regions of $RERG_{\text{vot}}$ for variant C_1 (a), and for variant C_2 (b)

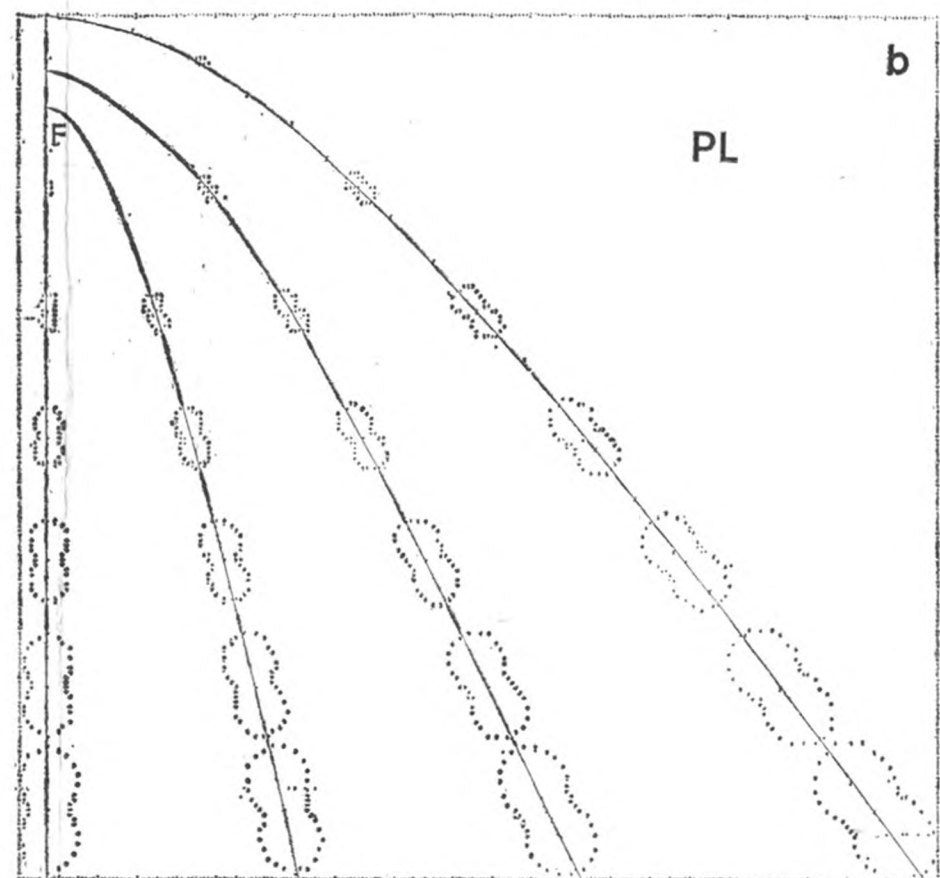
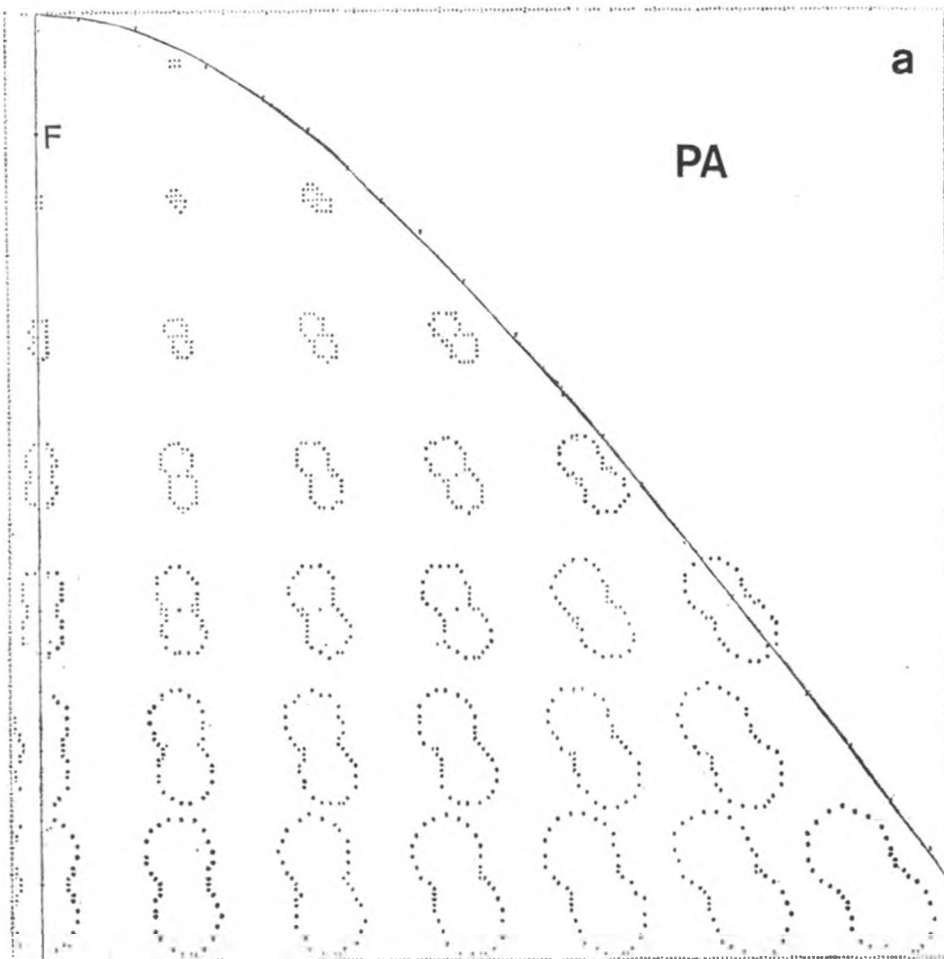


Fig. 10. Spatial and orientational variation of $RERG_1$ for variant C_2

Variant B₂ (Figs. 7 and 6b): $REG_{periclinat}$ on the axis increases linearly with physical distance from the focus

It is convenient to locate the origin of the z -axis at the focus and to take the focal length as a unit length. The physical distance from the focus, z , is then given on the axis by $z=1-\cos \eta$. From general form of the growth tensor we have on the axis $REG_{I(\eta)} = \frac{1}{\sin \eta} \frac{\delta V_n}{\delta \eta}$. By introducing the condition $REG_{I(\eta, z=0)} = k(1-\cos \eta)$ and integrating, we obtain $\bar{V}_n = -k \cos \eta - \frac{k}{2} \sin^2 \eta + c$ (on the axis). At the focus $\eta=0$, $\bar{V}_n=0$, $c=k$. Therefore, on the axis $\bar{V}_n = k(1-\cos \eta - \frac{1}{2} \sin^2 \eta)$ and in the whole dome $V_n = \frac{\sqrt{\sin^2 h^2 \xi + \sin^2 \eta}}{\sin \eta} k(1-\cos \eta - \frac{1}{2} \sin^2 \eta)$. The appropriate growth tensor thus is:

$$k \begin{pmatrix} (1-\cos \eta) - \frac{\cos \eta \sin h^2 \xi}{\sin h^2 \xi + \sin^2 \eta} \left(\frac{1}{1+\cos \eta} - \frac{1}{2} \right); \sin \eta \frac{\sin h \xi \cos h \xi}{\sin h^2 \xi + \sin^2 \eta} \left(\frac{1}{1+\cos \eta} - \frac{1}{2} \right); 0 \\ -\sin \eta \frac{\sin h \xi \cos h \xi}{\sin h^2 \xi + \sin^2 \eta} \left(\frac{1}{1+\cos \eta} - \frac{1}{2} \right); \sin^2 \eta \frac{\cos \eta}{\sin h^2 \xi + \sin^2 \eta} \left(\frac{1}{1+\cos \eta} - \frac{1}{2} \right); 0 \\ 0 \qquad \qquad \qquad 0 \qquad \qquad \qquad \cos \eta \left(\frac{1}{1+\cos \eta} - \frac{1}{2} \right) \end{pmatrix}$$

Inspection of this growth tensor indicates that the principal growth rates vanish at the vertex. Figs. 7a, b show the variation of linear growth rates in the planes PA and PL , and Fig. 6b shows the variation of the volumetric growth rate.

There are minima of all growth rates in the distal part of the dome. The maximal principal growth rate is in periclinal direction. This growth rate is well differentiated from the two remaining principal rates. The borders between the regions distinguished on the basis of the rate of volumetric growth run along anticlines.

HYPERBOLIC DOME

Variant C₁ (Figs. 8 and 9a): $REG_{periclinat} = REG_{I(\xi)}$ is constant along the axis

At the periclinal part of the axis $\eta=0$. From the general form of the growth tensor we have $REG_{I(\xi, z, n=0)} = \frac{1}{\sin h \xi} \frac{\delta V_\xi}{\delta \xi} = k$ on the axis. By integrating we obtain $\bar{V}_\xi = k(\cos h \xi - 1)$ (on the axis). Thus, in the whole dome we have $V_\xi = \frac{\sqrt{\sin^2 h^2 \xi + \sin^2 \eta}}{\sin h \xi} k(\cos h \xi - 1)$ and the growth tensor attains the particular form:

$$\frac{k}{\sin h^2 \xi + \sin^2 \eta} \left| \begin{array}{cc|c} \frac{\sin^2 \eta}{\cos h\xi + 1} + \sin h^2 \xi; & -\frac{\sin \eta \cos \eta (\cos h\xi - 1)}{\sin h\xi}; & 0 \\ \frac{\sin \eta \cos \eta (\cos h\xi - 1)}{\sin h\xi}; & \cos h\xi (\cos h\xi - 1); & 0 \\ 0 & 0 & \frac{\cos h\xi}{1 + \cos h\xi} (\sin h^2 \xi + \sin^2 \eta) \end{array} \right|$$

From this tensor we can see that at the vertex, where $\xi=0$ and $\eta>0$, the meridional and latitudinal principal growth rates are different from 0 and their ratio is 1. Maps of growth rate variations for this variant are given in Figs. 8 and 9a. The anisotropy of growth is nowhere very pronounced, the volumetric growth rate varies within a rather narrow range with the minimum being in the surface layer in the distal part.

Variant C₂ (Figs. 9b and 10): $REG_{periclinat} \equiv REG_{I(\xi)}$ increases linearly with physical distance from the focus

On the axis, $\eta=0$, the physical distance is $z = \cos h\xi - 1$ and the $REG_{I(\xi, \eta=0)} = \frac{1}{\sin h\xi} \frac{\delta V_\xi}{\delta \xi}$. Upon integration we obtain $\tilde{V}_\xi = k \left(\frac{1}{4} \cos h 2\xi - \cos h\xi \right) + C$.

At the focus $\xi=0$, $\tilde{V}_\xi=0$, thus $c = \frac{3}{4} k$. The displacement velocity for $k=1$ is:

$$\tilde{V}_\xi = \frac{1}{4} \cos h^2 \xi - \cos h\xi + \frac{3}{4} \text{ on the axis, and}$$

$$V_\xi = \frac{\sqrt{\sin h^2 \xi + \sin^2 \eta}}{\sin h\xi} \left(\frac{1}{4} \cos h 2\xi - \cos h\xi + \frac{3}{4} \right) \text{ in the whole dome.}$$

The growth tensor is:

$$\left(\frac{1}{4} \cos h 2\xi - \cos h\xi + \frac{3}{4} \right) \left| \begin{array}{cc|c} \frac{\cos h\xi - 1}{\frac{1}{4} \cos h 2\xi - \cos h\xi + \frac{3}{4}} - \frac{\cos h\xi \sin^2 \eta}{\sin h^2 \xi + \sin^2 \eta}; & 0 \\ -\frac{\sin \eta \cos \eta}{\sin h\xi (\sin h^2 \xi + \sin^2 \eta)}; & 0 \\ \frac{\sin \eta \cos \eta}{\sin h\xi (\sin h^2 \xi + \sin^2 \eta)}; & \frac{\cos h\xi}{\sin h^2 \xi + \sin^2 \eta}; & 0 \\ 0 & 0 & \frac{\cos h\xi}{\sin h^2 \xi} \end{array} \right|$$

The maps of $REG_{I(\xi)}$ and REG_{vol} are shown in Figs. 10 and 9b. The spatial variation of growth rates is similar to that in the variant A₂ for the parabolic dome.

DISCUSSION

As long ago as 1879 J. Sachs considered orthogonal periclinal and anticlinal trajectories in the form of confocal parabolas, ellipses and hyperbolas as a reference framework for the analysis of growth and cell divisions in apical meristems. This framework was most thoroughly exploited by Schüepp (1966), but still not as coordinate system. Schüepp's analysis of growth was not based on the mathematical concept of the derivative, thus curvilinear coordinate systems were irrelevant for him. The use of the periclinal and anticlinal as a natural coordinate system is, however, of basis importance in the type of growth analysis pioneered by Erickson and Sax (1956) which is applicable to organs such as apical domes. How to use the natural coordinate system in growth analysis is the problem dealt with in this paper, which is only a step towards the analysis of real meristems.

In the present paper we consider only two variants of growth distribution in apical domes growing with steady geometry. In both variants there is a strong tendency towards lower growth rates in the distal region of the dome. Such a tendency is manifested by shoot apices in angiosperms in the vegetative phase (Lynd on 1976). It seems probable that growth distributions in real domes is within the range delimited by the two variants considered here, or is not far from this range. Among the two variants the second seems more realistic. It is characterized by pronounced increasing of growth rates with distance from the vertex. For this variant the zones distinguished by volumetric growth rate are delineated by anticlinal surfaces, as also happens in real shoot apices. On the other hand, the lowering of the growth rates in the distal part of the dome in the case of the 2nd variant is more pronounced than usually happens in shoot apices of many species. Thus some combination of both variants is probably more realistic than either of the variant separately. Probably even better would be a model based on more complicated growth rate variation along the axis than the two simple cases considered here. Perhaps the modeling of growth in the shoot apex should be based on growth distribution specified for a displacement line on dome surface rather than on the axis. We have been aware of this possibility because it was indicated by the studies of Green (1980), however, in the first trial of the modeling based on the growth tensor we deliberately used the specification on dome axis because the modeling is in this case the simplest, and purpose of this paper was to provide an example of such modeling.

Acknowledgment

We express our thanks to Dr. J. A. Romberger for valuable advices, comments, and writing certain passages of the text.

REFERENCES

- Erickson R. O., 1976. Modeling of plant growth. *Ann. Rev. Plant Physiol.* 27: 407-434.
Erickson R. O., Sax K. B., 1956. Elemental growth rate of the primary root of *Zea mays*. *Proc. Amer. Phil. Soc.* 100: 487-498.

- Green P. B., 1980. Organogenesis — a biophysical view. *Ann. Rev. Plant Physiol.* 31: 51-82.
- Hejnowicz Z., 1984. Trajectories of principal direction of growth, natural coordinate system in growing plant organ. *Acta Soc. Bot. Pol.* 53: 000-000.
- Hejnowicz Z., Romberger J. A., 1984. Growth tensor of plant organs. *J. Theor. Biol.* (in press).
- Lyndon R. F., 1976. The shoot apex. In: *Cell Division in Higher Plants*. M. M. Yeoman (ed.). Academic Press, London. pp. 285-314.
- Sachs J., 1879. Ueber Zellenanordnung und Wachstum. *Arb. Bot. Inst. in Würzburg II Heft 2*: 185-208.
- Schüpp O., 1966. Meristeme, Wachstum und Formbildung in dem Teilungsgewebe höheren Pflanzen. Birkhauser Verlag, Basel.

Modelowanie przestrzennej zmienności wzrostu w apikalnych częściach wierzchołków pędu za pomocą tensora wzrostu

S t r e s z c z e n i e

Do opisu wzrostu organów roślinnych za pomocą tensora wzrostu stosować można naturalne układy współrzędnych. Ich wybór zależy od trajektorii głównych kierunków wzrostu w organie. Znajomość tensora wzrostu w naturalnym układzie współrzędnych jest wygodna do badań przestrzennej zmienności wzrostu. Względne elementarne szybkości wzrostu liniowego (REG_l) w kierunkach głównych są wtedy składowymi diagonalnymi tensora. Suma składowych diagonalnych stanowi względną szybkość wzrostu objętościowego (REG_{vol}). W pracy pokazano w jaki sposób stosować tensor wzrostu i naturalne układy współrzędnych do opisu apikalnych części wierzchołków pędu w przypadkach kiedy geometria wierzchołków nie zmienia się podczas wzrostu. Zbadano trzy typy wierzchołków: paraboliczny, eliptyczny i hiperboliczny. Przyjęto, że naturalnymi układami współrzędnych są: układ paraboloidalny dla wierzchołka parabolicznego oraz wydłużony sferoidalny dla eliptycznego i hiperbolicznego. Tensory wyznaczono dla dwóch wariantów REG_l na osi: stałej szybkości wzrostu i wzrastającej proporcjonalnie z odległością od ogniska układu współrzędnych. Przy pomocy komputera obliczono zmienność REG_l i REG_{vol} ilustrując ją mapami. W obu wariantach szybkości wzrostu są mniejsze w regionie dystalnym wierzchołka.